

In-medium Production of Kaons at the Mean-Field Level

Jürgen Schaffner^a, Jakob Bondorf^a, and Igor N. Mishustin^{a,b}

^a*The Niels Bohr Institute, Blegdamsvej 17, DK-2100 Copenhagen*

^b*The Kurchatov Institute Russian Research Center, Moscow 123182*

Abstract

The in-medium mass and energy of kaons and antikaons are studied within the Relativistic Mean Field approach and compared with predictions from chiral models by taking care of kaon-nucleon scattering data. Implications for the subthreshold production of kaons and antikaons in heavy-ion collisions are discussed. We find only small corrections due to in-medium effects on the mean-field level for the relevant production processes for kaons. The production of kaons is even less favourable at high density due to repulsive vector interactions. We conclude that one has to go beyond mean-field approaches and take fluctuations and secondary production processes into account to explain the recently measured enhancement of kaon production at subthreshold energies. The situation is different for antikaons where in-medium effects strongly enhances their production rates. We also see strong in-medium modifications of the annihilation processes of antikaons and Λ 's which might be visible in flow measurements. At high density, we predict that the threshold energy for antikaon and Λ production and annihilation become equal leading to similar numbers of antikaons and Λ 's in the dense zone of a relativistic heavy ion collision.

I. INTRODUCTION

In-medium properties of hadrons have received considerable attention recently, both experimentally and theoretically by studying relativistic heavy-ion collisions. Charged kaons (K^+) seem to be a quite promising tool for probing the dense interior of the collision zone as their mean free path is long enough to escape without further interactions. Kaplan and Nelson proposed first that a kaon condensed phase may be formed in the dense matter created in heavy ion collisions [1]. Further studies within the Nambu–Jona-Lasinio model [2], chiral perturbation theory [3] and an one-boson exchange model [4] showed that the kaon (K^+) sees a repulsive potential in the medium and will not condense.

On the other side, the antikaon (K^-) feels a strong attraction which is confirmed by recent calculations taking into account the contribution coming from the $\Lambda(1405)$ resonance just below threshold [5,6]. It was then predicted by chiral perturbation theory that a antikaon condensed phase will form in the dense interior of a neutron star [7] consistent with scattering data [3,8] and Kaonic atoms [9]. This approach has been criticised in [4,10] as the scalar density is set equal to the baryon density and higher order terms in density are neglected. The appearance of hyperons [11] shifts also the onset of a condensed phase to higher density. As shown in [12] a strong nonlinear dependence on density and the implementation of hyperon-hyperon interactions even prevents an antikaon condensed phase inside a neutron star.

Here we will continue our work for neutron stars [12] and apply it for the situation in heavy ion collisions at threshold. Subthreshold production rates of K^+ in heavy-ion reactions were recently measured at GSI [13]. Earlier work showed that the in-medium modifications of kaons and antikaons might be measurable in heavy ion collisions at threshold. For example, it was shown that the kaons are sensitive to the equation of state (EOS) [14–16]. A softer EOS produces more kaons than a hard one. On the other hand it will also depend on the parametrisation used for the cross section [17,18] but not on N-body collisions [19] and not on the high-momentum tail of the nucleons [20]. The influence of rescattering and formation

of resonance (Δ) matter was studied in the QMD model [15], and the RBUU model [21] and it was demonstrated that they are essential to explain the data. In-medium modifications of the effective energy of the kaon were studied in [22] using again the RBUU model. The results are essential similar to the ones obtained without medium modifications [21], because the in-medium kaon mass used is quite close to the respective vacuum mass. But there exist other observables which might be better suited for extracting in-medium effects. The flow of kaons might be a promising tool for measuring the kaon potential in dense matter [23]. And more pronounced in-medium effects are expected for the case of K^- [24]. Indeed, enhanced production rates for K^- have been seen at GSI recently [25].

In this paper we want to examine the possible influence of a dense nuclear environment on the properties of kaons and antikaons. We show that the in-medium effects on the mean-field level can not explain the measured enhanced production rates of kaons in contrary to the conclusion drawn in ref. [24]. We discuss two different approaches: first an one-boson exchange model and second a chiral approach where the parameters are fixed by s-wave scattering lengths and the low density theorem. In-medium effects for Λ 's are also taken into account by linking them to hypernuclear data. We show that the phase space in the medium does not change considerably for the processes $NN \rightarrow N\Lambda K$ and secondary processes as $\pi N \rightarrow \Lambda K$ and $N\Delta \rightarrow N\Lambda K$ due to cancelation effects. On the contrary, effects nonlinear in density even cause an enhanced repulsion at highly dense matter for these processes. Hence, subthreshold production of kaons seems *not* to probe the potentials of the very dense region of a heavy-ion collision. On the other hand, in-medium effects are essential for explaining the enhanced production of antikaons. We show that the process $NN \rightarrow NNK\bar{K}$ is enhanced in the medium while the annihilation process $\bar{K}N \rightarrow \Lambda\pi$ is reduced. We also find that the annihilation process $\Lambda N \rightarrow NN\bar{K}$ is essentially enhanced in dense matter and might be equally important as antikaon annihilation. This behaviour may lead to equal numbers of antikaons and Λ 's in the dense zone of a relativistic heavy ion collision.

The paper is organized as follows: first we introduce the Relativistic Mean Field (RMF) model and extend it to include Λ 's. In the second section we discuss two different interaction

schemes for the kaons with nuclear matter, one based on an one-boson exchange model and the other on chiral perturbation theory (ChPT). The parameters are fixed to the s-wave KN scattering lengths. Results for the in-medium effects on kaon and antikaon production are presented in the third section. The last section is devoted to conclusions and an outlook.

II. THE RMF MODEL

The RMF model has been proven to give a good description of nuclear matter in bulk and of the properties of finite nuclei [26,27]. We start from the Lagrangian

$$\begin{aligned} \mathcal{L} = & \bar{\Psi}_N(i\gamma^\mu\partial_\mu - m_N)\Psi_N + \frac{1}{2}\partial^\mu\sigma\partial_\mu\sigma - U(\sigma) \\ & - \frac{1}{4}G^{\mu\nu}G_{\mu\nu} + \frac{1}{2}m_\omega^2V^\mu V_\mu - \frac{1}{4}\vec{B}^{\mu\nu}\vec{B}_{\mu\nu} + \frac{1}{2}m_\rho^2\vec{R}^\mu\vec{R}_\mu \\ & - g_{\sigma N}\bar{\Psi}_N\Psi_N\sigma - g_{\omega B}\bar{\Psi}_N\gamma^\mu\Psi_NV_\mu - g_{\rho N}\bar{\Psi}_N\gamma^\mu\vec{\tau}\Psi_N\vec{R}_\mu \end{aligned} \quad (1)$$

where the nucleons interact via an attractive scalar (σ) and a repulsive vector (V^μ) meson field. The term $U(\sigma)$ stands for the scalar selfinteraction

$$U(\sigma) = \frac{1}{2}m_\sigma^2\sigma^2 + \frac{b}{3}\sigma^3 + \frac{c}{4}\sigma^4 \quad (2)$$

introduced by Boguta and Bodmer [28] to get a correct compressibility of nuclear matter (for another stabilized functional form see [29]). The parameters of this Lagrangian can be fixed to bulk properties [28] or to the properties of finite nuclei [30,31]. A general discussion about the scalar selfinteraction terms can be found in [32]. Bodmer proposed an additional selfinteraction term for the vector field [33]

$$\mathcal{L}_{V^4} = \frac{1}{4}d(V_\mu V^\mu)^2 \quad (3)$$

which leads to a soft equation of state at high densities in agreement with Dirac-Brückner calculations [33,34]. Fits to the properties of nuclei with this new term are quite successful [35]. In the following we take mostly the parameter sets NL-Z [30] which is the commonly

used parameter set NL1 with a better zero-point energy correction and the recent set TM1 [35] with vector selfinteraction terms. The former one gives a rather stiff equation of state while the latter one a rather soft one.

The implementation of hyperons proceeds as

$$\mathcal{L}_\Lambda = \bar{\Psi}_\Lambda(i\gamma^\mu\partial_\mu - m_\Lambda)\Psi_\Lambda - g_{\sigma\Lambda}\bar{\Psi}_\Lambda\Psi_\Lambda\sigma - g_{\omega\Lambda}\bar{\Psi}_\Lambda\gamma^\mu\Psi_\Lambda V_\mu \quad (4)$$

and the two new coupling constants can be fixed to hypernuclear data [36]. The main feature of hypernuclei is that the depth of the Λ -potential is about

$$U_\Lambda^{(N)} = g_{\sigma\Lambda}\sigma^{\text{eq.}} + g_{\omega\Lambda}V_0^{\text{eq.}} \approx -30 \text{ MeV} \quad (5)$$

in saturated nuclear matter which already fixes one coupling constant of the Λ , say $g_{\sigma\Lambda}$ [37,38]. The vector coupling constant $g_{\omega\Lambda}$ is then given by

$$g_{\omega\Lambda} = \frac{2}{3}g_{\omega N} \quad (6)$$

when using SU(6)-symmetry (the quark model, see e.g. [39]). The SU(6)-symmetry also secures that the spin-orbit force is negligible small as there is no experimental evidence for a spin-orbit splitting for hypernuclear levels. Noble showed first [40] that the contribution of the vector terms to the spin-orbit term nearly cancel each other when taking into account the tensor force and SU(6)-symmetry. The tensor force vanishes in bulk matter on the mean field level as it is proportional to the gradient of the fields. Therefore it is not considered here.

The in-medium energy of nucleons and hyperons is then given by

$$E_N(p) = \sqrt{(m_N + g_{\sigma N}\sigma)^2 + p^2} + g_{\omega N}V_0 + g_{\rho N}\tau_0 R_{0,0} \quad (7)$$

$$E_\Lambda(p) = \sqrt{(m_\Lambda + g_{\sigma\Lambda}\sigma)^2 + p^2} + g_{\omega\Lambda}V_0 \quad (8)$$

It is important to note that the parameters here are connected to properties at normal nuclear matter density. The in-medium effects for nucleons and Λ 's at this point are known and should be taken into account when studying the influences and the signals of a dense

nuclear environment. As pointed out in [41] three-body forces are also important to explain hypernuclear data. As these forces are repulsive, the hyperon potential shows a nonlinear behaviour with density and changes sign at higher density. Figure 1 shows the Schrödinger equivalent potential defined as

$$U_{\text{SEV}} = g_{\sigma\Lambda}\sigma + g_{\omega\Lambda}V_0 + \frac{1}{2m_\Lambda} \left((g_{\sigma\Lambda}\sigma)^2 - (g_{\omega\Lambda}V_0)^2 \right) \quad (9)$$

for different parameter sets in comparison with the findings of the non-relativistic approach [41]. The overall behaviour is quite similar despite of the EOS used. The nonlinear behaviour of the scalar field with density seems to simulate the repulsive three-body force of the nonrelativistic approach. It also demonstrate that is crucial to make a difference between scalar and vector (baryon) density. This turning of the hyperon potential will be quite important for our discussion of the kaon production in the medium.

III. KAON INTERACTIONS

The case for the kaon is quite distinct from that of the Λ . There does not exist any kaon-nuclear states similar to hypernuclei as the KN-interaction is known to be repulsive. Taking the (real) isospin averaged KN-scattering length $\bar{a}_{KN} = (3a_0^{I=1} + a_0^{I=0})/4 = -0.255$ fm [42] and using the low density theorem one gets a repulsive optical potential depth at normal nuclear density of about

$$U_{\text{opt}}^{\text{KN}} = -\frac{2\pi}{m_K} \left(1 + \frac{m_K}{m_N} \right) \bar{a}_{KN} \rho_N \approx +29 \text{ MeV } \rho_N / \rho_0 \quad (10)$$

compatible with kaon (K^+) scattering on nuclear targets [39]. Here we have taken the groundstate density to be $\rho_0 = 0.15 \text{ fm}^{-3}$. The repulsive interaction is the reason why kaons have a long mean-free path in nuclear matter. Note that the potential depth is just opposite to the one of the Λ which signals a significant cancellation of attractive and repulsive terms in the medium. On the other hand, a recent experiment measured an enhanced cross section for K^+ scattering on nuclear targets [43] incompatible with multiple

scattering arguments. This is the so called K^+ -puzzle which is still unresolved. The isospin dependent potential in nuclear matter can be estimated from the isospin scattering length $a_{\text{iso}} = (a_0^{I=1} - a_0^{I=0})/4 = -0.055$ fm and the low density theorem

$$U_{\text{iso}}^{\text{KN}} = -\frac{2\pi}{m_K} \left(1 + \frac{m_K}{m_N}\right) \bar{a}_{\text{iso}} \rho_{\text{iso}} \approx +6 \text{ MeV } \rho_{\text{iso}}/\rho_0 \quad (11)$$

where ρ_{iso} is the isospin density of the system. For lead one can estimate $\rho_{\text{iso}} \approx (2Z - A)/A\rho_N \approx -0.21\rho_N$, which gives about 1 MeV correction at normal nuclear density.

For antikaons the annihilation processes

$$\bar{K} + N \rightarrow Y + \pi \quad (Y = \Lambda, \Sigma) \quad (12)$$

gives a big imaginary part for the scattering lengths. At first glance the experimental situation seems to be contradictory: The available K^- -N-scattering indicates a repulsive interaction while the K^- -atomic data demands an attractive potential. The situation can be remedied by taking care of the existence of the $\Lambda(1405)$ -resonance just below threshold. Recently an improved fit of K^- -atomic data was carried out assuming a nonlinear density dependence of the effective t -matrix [44]. It has been shown that the real part of the antikaon optical potential can be as attractive as

$$U_{\text{opt}}^{\bar{K}N} \approx -200 \pm 20 \text{ MeV} \quad (13)$$

at normal nuclear matter density while being slightly repulsive at very low densities in accordance with K^- -p-scattering. The change of the sign and the nonlinear density dependence results from the $\Lambda(1405)$ -resonance. Also another family of solutions have been found with a moderate potential depth around -50 MeV. Note that also the standard linear extrapolation gives only values of about -85 MeV [44]. These latter two solutions are not getting repulsive at low densities, i.e. fulfilling the low-density theorem.

The K^- -N-scattering data can be explained by vector meson exchange models where the $\Lambda(1405)$ is a quasi-bound state in the t -channel [45,46]. In a recent paper the coupled channel analysis of Siegel and Weise [45] has been also applied for interactions terms coming from

chiral perturbation theory [47]. The coupled channel formalism automatically generates the $\Lambda(1405)$ and successfully describes the low energy K^-p -scattering data.

In the following we adopt the meson-exchange picture and the chiral approach for the KN-interaction on the mean-field level and fix the parameters to the KN-scattering length. The case for the antikaons is then given by a G-parity transformation which simply changes the sign of the vector potential term. This simple treatment does not take care of the important contribution of the $\Lambda(1405)$ resonance. But there exist some hints that this resonance seems to be less important in dense matter (which happens when the antikaon energy is shifted down below $m(\Lambda(1405)) - m_N \approx 466$ MeV). In ref. [5] a separable potential was applied for the K^-p -interaction for finite density. Indeed, it was found that the mass of the $\Lambda(1405)$ is shifted upwards and exceeds the K^-p threshold already at densities of about $\rho \approx 0.4\rho_0$. This is supported by recent findings within a chiral approach [6], where this resonance vanishes at very low densities $\rho \approx 0.2\rho_0$ due to Pauli-blocking effects. In this case the use of mean-field potentials may be justified. Hence, we simplify our calculation by neglecting the contributions coming from the $\Lambda(1405)$ in the medium and treat the problem on the tree-level using G-parity. Nevertheless, the results presented for the $NN \rightarrow NN\bar{K}K$ case should be taken with some care. More elaborated models are needed to draw final conclusions about the in-medium property of antikaons in the medium.

A. One boson-exchange approach

We start from the following Lagrangian [12]

$$\mathcal{L}_{KN} = D_\mu^* \bar{K} D^\mu K - m_K^2 \bar{K} K - g_{\sigma K} m_K \bar{K} K \sigma - g_{\delta K} m_K \bar{K} \vec{\tau} K \vec{\delta} \quad (14)$$

with the covariant derivative

$$D_\mu = \partial_\mu + ig_{\omega K} V_\mu + ig_{\rho K} \vec{\tau} \vec{R}_\mu \quad . \quad (15)$$

For completeness we also add isospin-dependent terms which couple to an isovector-scalar field (δ) and an isovector-vector field (R_μ). Note that interaction terms of the form

$$\mathcal{L}_{KN\Lambda} = -g_{KN\Lambda} \left(\bar{N} \tau \gamma_5 \Lambda K + \bar{\Lambda} \tau \gamma_5 N \bar{K} \right) \quad (16)$$

do not contribute on the mean-field level as they are off-diagonal terms. We will come to this point later in more detail.

The coupling constants to the vector mesons are chosen from the SU(3)-relations assuming ideal mixing

$$2g_{\omega K} = 2g_{\rho K} = g_{\pi\pi\rho} = 6.04 \quad (17)$$

where $g_{\pi\pi\rho}$ is fixed by the ρ decay width. The scalar coupling constants can be fixed to the s-wave KN-scattering lengths [12]. The isospin averaged scattering length in the tree approximation is given by [48]

$$\bar{a}_{KN} = \frac{1}{4}a_0^{I=0} + \frac{3}{4}a_0^{I=1} = \frac{m_K}{4\pi(1+m_K/m_N)} \left(\frac{g_{\sigma K}g_{\sigma N}}{m_\sigma^2} - 2\frac{g_{\omega K}g_{\omega N}}{m_\omega^2} \right) = -0.255 \text{ fm} \quad (18)$$

where only the isoscalar terms contribute. This can be used to fix $g_{\sigma K}$ for known $g_{\omega K} = 3.02$.

The KN-scattering lengths for a given Isospin I on the tree level are then given by [48]

$$a_0^{I=1} = \frac{m_K}{4\pi(1+m_K/m_N)} \left(\frac{g_{\sigma K}g_{\sigma N}}{m_\sigma^2} + \frac{g_{\delta K}g_{\delta N}}{m_\delta^2} - 2\frac{g_{\omega K}g_{\omega N}}{m_\omega^2} - 2\frac{g_{\rho K}g_{\rho N}}{m_\rho^2} \right) \quad (19)$$

$$a_0^{I=0} = \frac{m_K}{4\pi(1+m_K/m_N)} \left(\frac{g_{\sigma K}g_{\sigma N}}{m_\sigma^2} - 3\frac{g_{\delta K}g_{\delta N}}{m_\delta^2} - 2\frac{g_{\omega K}g_{\omega N}}{m_\omega^2} + 6\frac{g_{\rho K}g_{\rho N}}{m_\rho^2} \right) \quad (20)$$

Recent experimental values are $a_0^{I=1} = 0.31$ fm and $a_0^{I=0} = -0.09$ fm [42]. The importance of the δ -meson exchange contribution can be seen by looking at the $a_0^{I=0}$ scattering length. The vector terms largely cancel each other as $g_{\omega K}g_{\omega N} \approx 3g_{\rho K}g_{\rho N}$. Hence, without the contribution from the δ -exchange one gets

$$a_0^{I=0} = \frac{m_K}{4\pi(1+m_K/m_N)} \left(\frac{g_{\sigma K}g_{\sigma N}}{m_\sigma^2} \right) \approx 0.4 \text{ fm} \quad (21)$$

in contradiction with experiment (here we used $g_{\sigma N} = 10$, $g_{\omega N} = 13$ as standard values for the RMF model). Including the δ -meson term and using $g_{\delta N} = 5.95$ from the Bonn model [49] one can fit both scattering lengths nicely for

$$g_{\sigma K} \approx 1.9 - 2.3, \quad g_{\delta K} \approx 5.6 - 6.4 \quad (22)$$

for the various nucleonic parameter sets used in the literature (see Table I). Note that the values of $g_{\sigma K}$ significantly deviate from the simple quark-model (simple quark counting gives $g_{\sigma K} = g_{\sigma N}/3 \approx 3.3$). The coupling of the kaon to the δ -meson is quite strong. Therefore, we expect some effects for isospin-asymmetric systems which we will discuss later.

The fit based on the adjustment to the KN-scattering lengths leads to an optical potential of

$$2m_K U_{\text{opt}}^{\bar{K}} = \omega_K^2 - m_K^2 = g_{\sigma K} \sigma m_K - 2g_{\omega K} \omega_{\bar{K}} V_0 - (g_{\omega K} V_0)^2 \quad (23)$$

which gives $U_{\text{opt}}^{\bar{K}} = -(85 \div 100)$ MeV at normal nuclear density for the parameter sets used. These values are lower than the ones quoted in our previous work [12] as we use here the vacuum kaon mass m_K instead of the reduced mass μ_{KN} . We think that this is more consistent with the parametrisation used in the study of Kaonic atoms [44], but now our value is much closer to the standard fit which gives $U_{\text{opt}}^{\bar{K}} = -85$ MeV. Note that the optical potential as defined in (23) is always lower than the relativistic potential the kaon feels at normal nuclear density which is about

$$U_{\text{rel}}^{\bar{K}} = \omega_{\bar{K}} - m_K \approx -(95 \div 110) \text{ MeV} \quad . \quad (24)$$

This definition corresponds to the sum of scalar and vector potentials as discussed in [50]. Nevertheless, the scalar and also the vector potential are much lower than the ones deduced from simple quark model counting as used in [50]. The reason is that our coupling ratios are about $g_{\sigma K}/g_{\sigma N} \approx 1/5$ and $g_{\omega K}/g_{\omega N} \approx 0.23$ (see Table I) which significantly deviates from the simple quark model value of $1/3$.

We have also studied the influences of off-shell terms which have only small influences on the in-medium behaviour of kaons (see [12]). Note that off-shell terms are not needed for describing the s-wave KN-scattering lengths correctly. On the other hand, they are essential for the chiral approach which we will discuss in the next section.

The equation of motion for kaons in the mean-field approximation in uniform matter reads

$$\left\{ \partial_\mu \partial^\mu + m_K^2 + g_{\sigma K} m_K \sigma + g_{\delta K} m_K \tau_0 \delta_0 + 2(g_{\omega K} V_0 + g_{\rho K} \tau_0 R_{0,0}) \right\} i \partial^\mu$$

$$-(g_{\omega K}V_0 + g_{\rho K}\tau_0 R_{0,0})^2\} K = 0 \quad . \quad (25)$$

Note that there appears terms quadratic in the vector fields in eq. (25). The importance of the isospin dependent terms can be estimated from the equation of motions for the vector fields in uniform matter

$$m_\omega^2 V_0 + dV_0^3 = g_{\omega N}\rho_N \quad (26)$$

$$m_\rho^2 R_{0,0} = g_{\rho N}(\rho_p - \rho_n) \quad (27)$$

where ρ_p and ρ_n are the densities of protons and neutrons, respectively. For lead one gets $\rho_p - \rho_n \approx (2Z - A)/A\rho_N \approx -0.21\rho_N$, and the isovector correction is then about

$$\frac{g_{\rho K}R_{0,0}}{g_{\omega K}V_0} \approx 21\% \frac{g_{\rho N}m_\omega^2}{g_{\omega N}m_\rho^2} \approx 8\%$$

if one neglects the vector field selfinteraction which holds for low densities. Hence, the isovector contributions are expected to be small for the densities considered here ($\rho < 3\rho_0$).

The effective mass of the kaon is given by

$$m_K^* = \sqrt{m_K^2 + m_K(g_{\sigma K}\sigma + g_{\delta K}\tau_0\delta)} \quad . \quad (28)$$

The scalar field σ reduces the effective mass of the kaon in the medium, i.e. the scalar interaction is attractive. The isovector-scalar field δ shifts the effective mass if there is an isospin asymmetry in the system. Note that for kaons as bosons the dependence on the scalar potential is different from that for nucleons (fermions): for low densities the reduction of the kaon mass in the medium is proportional to the square root of the scalar attraction while it is linear for the case of baryons (see eq. (7)). Moreover we point out that the scalar potentials always follow the *scalar* density as demanded by Lorentz invariance. The scalar density is saturating in dense matter to ensure the existence of a saturation point of the equation of state. As shown in [4,10] these nonlinear effects are important already at a moderate density and causes a saturation of the effective kaon mass with density. We can even go further and say that there exists a minimum effective kaon mass. As the effective

mass of the nucleon approaches zero at high density ($m_N^* \rightarrow 0$) in the Walecka model, the minimum scalar field is about $\sigma_{min} = -m_N/g_{\sigma N}$ and one gets for the minimum effective kaon mass

$$m_{K,min}^* = \sqrt{m_K^2 + m_K g_{\sigma K} \sigma_{min}} \approx \sqrt{m_K^2 + \frac{m_K g_{\sigma K}}{m_N g_{\sigma N}}} \approx 390 \text{ MeV} \quad (29)$$

for the parameters of Table I.

Decomposing the kaon field into plane waves one obtains the following dispersion relation for kaons (upper sign) and antikaons (lower sign) in uniform matter composed of nucleons only

$$\omega_{K,\bar{K}} = \sqrt{m_K^*{}^2 + k^2} \pm (g_{\omega K} V_0 + g_{\rho K} \tau_0 R_{0,0}) \quad . \quad (30)$$

Note that due to the covariant derivative coupling scheme (15) the vector term appears linearly in the kaon energy. The vector field is repulsive (attractive) for the kaon (antikaon) and will dominate the behaviour in very dense matter. For high density the kaon (antikaon) energy is then increasing (decreasing) as $\rho^{1/3}$ because the vector field is growing with $\rho^{1/3}$ if one takes into account the vector field selfinteraction term (see eq. (26)). Otherwise it is changing linear in density.

B. Chiral Approach

We follow the procedure outlined in [3] starting from the Nonlinear Chiral Lagrangian in next-to-leading order

$$\begin{aligned} \mathcal{L}_{KN}^{chiral} = & -\frac{3i}{8f_K^2} \left[\bar{N} \gamma_\mu N \left(\bar{K} \overleftrightarrow{\partial}^\mu K \right) + \bar{N} \vec{\tau} \gamma_\mu N \left(\bar{K} \vec{\tau} \overleftrightarrow{\partial}^\mu K \right) \right] \\ & + \frac{\Sigma_{KN}}{f_K^2} \bar{N} N \bar{K} K + \frac{C}{f_K^2} \bar{N} \vec{\tau} N \bar{K} \vec{\tau} K \\ & + \frac{\tilde{D}}{f_K^2} \bar{N} N \left(\partial_\mu \bar{K} \partial^\mu K \right) + \frac{\tilde{D}'}{f_K^2} \bar{N} \vec{\tau} N \left(\partial_\mu \bar{K} \vec{\tau} \partial^\mu K \right) \end{aligned} \quad (31)$$

where $f_K = 93 \text{ MeV}$ is the kaon decay constant and Σ_{KN} is the KN sigma term. The first two terms are the Tomozawa–Weinberg terms and are in leading order of the chiral expansion. These are vector interactions terms and repulsive (attractive) for kaons (antikaons).

The other terms are in next-to-leading order. The next two terms are scalar interactions which will decrease the effective mass of the kaon and antikaon. The last two terms are the so called off-shell terms which will modify the scalar attraction. Here one encounters striking similarity with the RMF model as the interaction is governed by scalar and vector interactions (see [50] for a discussion about this point). In the original paper [3] the authors choose $\Sigma_{KN} \approx 2m_\pi$ in accordance with the Bonn model [46]. More recently the value $\Sigma_{KN} = 450 \pm 30$ MeV is favoured according to lattice gauge calculations [51]. The constant C can be fixed from the Gell-Mann–Okubo mass formula to $C = 33.5$ MeV. The corresponding scattering lengths

$$\begin{aligned} a_{I=1}^{KN} &= \frac{1}{4\pi f_K^2 (1 + m_K/m_N)} \left[-m_K + \Sigma_{KN} + C + (\tilde{D} + \tilde{D}') m_K^2 \right] \\ a_{I=0}^{KN} &= \frac{1}{4\pi f_K^2 (1 + m_K/m_N)} \left[+\Sigma_{KN} - 3C + (\tilde{D} - 3\tilde{D}') m_K^2 \right] \end{aligned} \quad (32)$$

determine the constants \tilde{D} and \tilde{D}' for a given Σ_{KN} via the relations

$$\tilde{D} \approx 0.33/m_K - \Sigma_{KN}/m_K^2, \quad \tilde{D}' \approx 0.16/m_K - C/m_K^2 \quad . \quad (33)$$

Note that the off-shell terms involving the constants \tilde{D} and \tilde{D}' are essential for a correct description of the scattering lengths (see [3] for details). The equation of motion in the mean-field approximation and in uniform matter reads

$$\begin{aligned} &\left(\partial_\mu \partial^\mu + m_K^2 - \frac{\Sigma_{KN}}{f_K^2} \rho_s - \frac{C}{f_K^2} \tau_0 \rho_s^{iso} \right. \\ &\left. + \frac{\tilde{D}}{f_K^2} \rho_s \partial_\mu \partial^\mu + \frac{\tilde{D}'}{f_K^2} \tau_0 \rho_s^{iso} \partial_\mu \partial^\mu + \frac{3i}{4f_K^2} \rho_N \partial_t + \frac{i}{4f_K^2} \tau_0 \rho_N^{iso} \partial_t \right) K = 0 \end{aligned} \quad (34)$$

where $\rho_s^{iso} = \rho_{s,p} - \rho_{s,n}$ is the scalar-isovector density and $\rho_N^{iso} = \rho_p - \rho_n$ the vector-isovector density which are simply the difference of the corresponding densities of protons and neutrons. The mass of the kaon is shifted by

$$m_K^* = \sqrt{m_K^2 - \frac{\Sigma_{KN}}{f_K^2} \rho_s - \frac{C}{f_K^2} \tau_0 \rho_s^{iso}} \quad (35)$$

and the same arguments as for the case of the one-boson exchange model holds. One sees again that the scalar potential for the kaon behaves differently as the one for nucleons (7).

More important is, that there exists a minimum effective kaon mass as a minimum scalar field implies a maximum scalar density for the Walecka model which is about $\rho_{s,max} \approx 2\rho_0$ (see e.g. [29]). This gives a minimum kaon effective mass of 350 – 400 MeV depending on the kaon-nucleon sigma term. The influence of the isovector terms can be estimated from isospin considerations: e.g. for lead one has $\rho_p - \rho_n \approx (2Z - A)/A\rho_N \approx -0.21\rho_N$, i.e. about $21/3 = 7\%$ correction for the vector-isovector term of eq. (34). This is in accordance with our estimate for the one-boson exchange model in the previous section. In the following we will neglect the isovector contributions. Fourier transformation of the equation of motion yields

$$-\omega^2 + k^2 + \Pi(\omega, k; \rho_N) = -\omega^2 + k^2 + m_K^2 - \frac{\Sigma_{KN}}{f_K^2} \rho_s - \frac{\tilde{D}}{f_K^2} \rho_s \omega^2 - \frac{3}{4f_K^2} \omega \rho_N = 0 \quad . \quad (36)$$

where $\Pi(\omega, k; \rho_N)$ is kaon self energy which depends in general also on the kaon energy. This has to be taken into account to get the energy of a kaon/antikaon in the nuclear medium

$$\omega_{K,\bar{K}} = \left[\sqrt{m_K^*{}^2 \left(1 + \frac{\tilde{D}}{f_K^2} \rho_s \right) + k^2 + \left(\frac{3}{8f_K^2} \rho_N \right)^2} \pm \frac{3}{8f_K^2} \rho_N \right] \left(1 + \frac{\tilde{D}}{f_K^2} \rho_s \right)^{-1} \quad , \quad (37)$$

where m_K^* is defined by eq. (35). Here we note that in the high density limit the kaon energy is growing linear with density while for the antikaon the energy saturates at m_K^* as the vector contributions cancel each other. The optical potential at normal nuclear density

$$U_{\text{opt}}^{\bar{K}} = \frac{1}{2m_K} \Pi(\omega_{\bar{K}}, k = 0; \rho_0) \approx -68 \text{ MeV} \quad (38)$$

is rather moderate while the relativistic potential is about -75 MeV. This is in contrast to the findings of Brown and Rho [50] who gets a rather deep potential of -200 MeV. There are several reasons for this discrepancy: first BR-scaling is not taken into account here (which gives an additional factor of $5/3$ at ρ_0 , i.e. a potential of -125 MeV), second Brown and Rho neglect the off-shell term and do not take into account the KN-scattering lengths, third they neglect the energy dependence of the kaon self energy, fourth they assume that the scalar and vector density are equal, fifth they neglect that the scalar potential of the kaon behaves differently in matter compared to the nucleon one (see the discussion of eq. (35) above).

IV. RESULTS

A. Kaon energy in matter

Recently, the dynamics of the $\Lambda(1405)$ has been studied in nuclear matter using a coupled channel formalism [5,6]. The most important finding is that the effects coming from the $\Lambda(1405)$ vanishes at rather low densities ($\rho < 0.25\rho_0$). The optical potential for the antikaon is about -100 MeV [5] and -107 MeV [6] corresponding to a kaon energy of $\omega_{\bar{K}} = 380$ MeV and $\omega_{\bar{K}} = 372$ MeV at normal nuclear density, respectively. These values are in accordance with the ones calculated in the mean field approximation in the previous sections within the relativistic mean field (RMF) model and the chiral perturbation theory (ChPT).

In the following we discuss the in-medium energy of kaons and antikaons in nuclear matter using a soft (set TM1 of Table I) and a hard (set NL-Z of Table I) equation of state. Figure 2 shows the energy of kaons (upper curves) and antikaons (lower curves) with the soft EOS for the RMF model (eq. (30)), ChPT (eq. (37)) and the results of the coupled channel analysis of Waas et al. [6]. In the case of ChPT we discuss three cases: i) for a sigma term of $\Sigma_{KN} = 2m_\pi$ as used in [3], ii) for a sigma term of $\Sigma_{KN} = 450$ MeV as derived from recent lattice data [51], iii) for vanishing off-shell terms (denoted as $\tilde{D} = 0$) and a sigma term of $\Sigma_{KN} = 2m_\pi$ as used as input for the RBUU calculations [16,22–24].

All models show a quite similar behaviour in Fig. 1 for the kaon energy at low density except for the case $\tilde{D} = 0$. This results from the low density theorem and is a generic feature when the coupling constants are fixed to the KN-scattering lengths. Neglecting the off-shell terms, i.e. setting $\tilde{D} = 0$, violates the low density theorem. This gives a slower raise of the kaon energy with density and the kaon energy nearly stays constant for a wide range of density. Note that this latter parametrisation for the kaon energy is used in the dynamical calculations [22]. For higher density the other curves also start to deviate. The ChPT gives a higher kaon mass, i.e. more repulsion than in the RMF model. The results of the coupled channel calculation seems to follow more closely the one of ChPT. At $\rho = 3\rho_0$ the kaon

energy reads $\omega_K = 585$ MeV for the RMF model, $\omega_K = 630$ MeV for the coupled channel analysis [6] and $\omega_K = 640 - 670$ MeV for ChPT, so they deviate about 85 MeV from each other.

The antikaon energy (lower curves) of the different models is always attractive, except for the small density region for the coupled channel calculations due to the $\Lambda(1405)$ resonance. The latter one gives the most attraction of about $\omega_{\bar{K}} = 217$ MeV at $\rho = 3\rho_0$, followed by the RMF model with $\omega_{\bar{K}} = 263$ MeV and the ChPT with $\omega_{\bar{K}} = 280 \div 300$ MeV. The curve for the case of $\tilde{D} = 0$ used in [24] follows closely the one for the RMF model. All the curves for the antikaon energy are lying surprisingly close together. Note that the prediction of ChPT is rather insensitive to the choice of Σ_{KN} but rather sensitive to the off-shell terms, especially for the kaon energy.

In Fig. 3 the case for the hard EOS is plotted. Now the curves of the kaon energy are lying very close together, even at higher densities. This is due to the fact that the vector potential in the RMF model is now raising linear with density as in the ChPT in contrary to the soft EOS where it raises like $\rho^{1/3}$ due to the vector self-interaction terms. The energy of the kaon is now between $\omega_K = 630 \div 670$ MeV at $\rho = 3\rho_0$. Without the off-shell terms, the kaon energy significantly deviates from the other curves and stays rather constant up to $1.5\rho_0$. Note that the overall changes for the hard EOS compared to the soft EOS are quite moderate, especially when using ChPT, and only show up at higher density.

The different predictions for the antikaon energy seems to split now into two regimes: the results for the ChPT give a antikaon energy of about $\omega_{\bar{K}} = 300$ MeV at $\rho = 3\rho_0$ rather independent of the off-shell term and the choice of Σ_{KN} , while the RMF model and the coupled channel analysis get around $\omega_{\bar{K}} = 200$ MeV at $\rho = 3\rho_0$. The antikaon energy within the RMF model is now much deeper due to the stronger vector potential compared to the soft EOS. We want to point out again, that Dirac-Brückner calculations seems to favour the soft EOS [33,34]. Nevertheless, we see that the differences in the kaon/antikaon energy due to the EOS are well within the differences of the model predictions.

B. Threshold energy for kaon production in matter

In the following we discuss the shift of the threshold energy of various processes for heavy ion collisions due to medium modifications.

Kaons are mainly produced at threshold via the process $NN \rightarrow N\Lambda K$. The minimum energy needed is $Q(N\Lambda K) \approx 671$ MeV in vacuum. In the medium, the threshold is shifted to

$$Q(N\Lambda K) = E_\Lambda(p = 0) + \omega_K(k = 0) - E_N(p = 0) \quad (39)$$

where we assume that the outgoing nucleon is not Pauli-blocked in the hot zone of the collision. Hence, the subthreshold production of kaons is sensitive to three different in-medium effects: the EOS (E_N), the Λ potential (E_Λ) and the kaon energy (ω_K) in medium. These effects will partly cancel each other as the kaon feels a repulsive potential of 29 MeV (eq. (10)) while the Λ sees an attractive potential of -30 MeV at ρ_0 (eq. (5)). Therefore, subthreshold kaon production seems to probe mainly the EOS. As the nucleons feel an attractive potential of about -60 MeV the threshold will be shifted *upwards* at normal nuclear density by this amount and the production of kaons is *reduced* in the medium. This is indeed the case as can be seen from Fig. 4 which shows the threshold energy $Q(N\Lambda K)$ as a function of density. The similar behaviour of the different curves at low density is due to the low-density theorem. At $\rho = 3\rho_0$ the value of $Q(N\Lambda K)$ reaches about 800 MeV for the RMF model and about 860 MeV for ChPT which is quite insensitive to the value of the sigma term. Without off-shell terms, the threshold energy is underestimated in medium, and we expect that the production rates for kaons calculated in [22,24] are overestimated. Note, that all calculations ignoring in-medium effects [15,21] will also give a too high production rate for kaons. The case for the hard EOS is plotted in Fig. 5. The behaviour of the threshold energy in medium is quite similar for the different EOS considered here. Again, the low density limit more or less fixes the shape of the curves of the kaon energy independent of the EOS used. The curves for the RMF model and ChPT are lying closely between 800 – 830 MeV at $\rho = 3\rho_0$. Especially, the curve for the RMF model does not change considerable

for the hard EOS compared to the soft one. All curves seem to saturate for the hard EOS but are lying within the uncertainties of the different models used for the kaon energy. A definite conclusion whether or not subthreshold kaon production probes the EOS can not be drawn until the in-medium properties of the kaon can be determined more precisely.

Antikaons are created in heavy ion collisions first by the process $NN \rightarrow NNK\bar{K}$. The threshold value of $Q(K\bar{K}) \approx 988$ MeV is modified in the medium by the sum of the kaon and antikaon energy $Q(K\bar{K}) = \omega_K(k=0) + \omega_{\bar{K}}(k=0)$. Therefore, subthreshold antikaon production probes the in-medium property of kaons and antikaons solely. As the vector potential cancels out approximately, it will mainly depend on the scalar potential the kaon feels in the medium. The upper curves in Fig. 4 show that indeed $Q(K\bar{K})$ is reduced in the medium in all models discussed here. ChPT predicts an in-medium reduction of about -56 MeV at maximum compared to the vacuum and then the curves go up again for higher density. The reason is that the sum of the kaon and antikaon energy contains a term coming from the Tomozawa–Weinberg term

$$\omega_K(k=0) + \omega_{\bar{K}}(k=0) = 2\sqrt{m_K^*{}^2 \left(1 + \frac{\tilde{D}}{f_K^2}\rho_s\right) + \left(\frac{3}{8f_K^2}\rho_N\right)^2 \left(1 + \frac{\tilde{D}}{f_K^2}\rho_s\right)^{-1}}, \quad (40)$$

which is repulsive and dominates at higher density. On the other side, the RMF model gives a reduction of about -140 MeV at $\rho = 3\rho_0$. The Q -value is steadily decreasing as the sum of the kaon and antikaon energy

$$\omega_K(k=0) + \omega_{\bar{K}}(k=0) = 2m_K^* = 2\sqrt{m_K^2 + m_K g_{\sigma K} \sigma} \quad (41)$$

depends on the attractive scalar potential only. The curve used in RBUU calculations with a soft EOS [24] is lying even lower and hence, the production rates of antikaons seems to be overestimated. Using the hard EOS (Fig. 5) the situation does not change significantly. The Q -value in the RMF model is now reduced by -160 MeV at $\rho = 3\rho_0$. The curves for the ChPT go up stronger at higher density compared to the soft EOS as they are sensitive to the strength of the vector potential (i.e. to the behaviour of the EOS at high density) in contrast to the RMF model.

As an interesting fact, the Q -values for kaon and antikaon production are lying close together for the RMF model. Note that this does not mean that the numbers of produced kaons and antikaons are the same inside the dense medium. The kaons will be produced at different density and the average Q -value over the density profile will give a measure for the produced kaons and antikaons in the medium. On the other hand, the production of kaons will be dominated by the secondary processes (rescattering effects) $N\Delta \rightarrow N\Lambda K$ and $\pi N \rightarrow \Lambda K$, the production of antikaons by the processes $N\Delta \rightarrow NNK\bar{K}$ and $\pi N \rightarrow K\bar{K}$. Let us assume that the change of the Δ mass and energy is equal to that of the nucleon. Then the Q -values of these channels can be simply derived by shifting the corresponding curves for the Q -values of Figs. 4 and 5 down by $m_N - m_\Delta \approx -290$ MeV (ignoring the finite width of the Δ) and by $-m_\pi$, respectively. If the Δ feels a higher (lower) potential than the nucleon, then this will suppress (enhance) subthreshold kaon production. Processes involving two Δ 's in the entrance channel will decrease the Q -value by -580 MeV compared to the two nucleon one and hence, enhanced production of kaons will be sensitive to Δ matter (density isomers) [15].

Also annihilation processes will play a dominant role at high density. Kaons will not annihilate and escape due to their long free mean path. But the charge exchange reaction $K^+n \rightarrow K^0p$ will act like an annihilation process for kaons as only charged particles are measured in the present heavy ion experiments [13]. This process will be modified in the medium only by isovector potentials. We do not expect changes of the threshold energy for isospin symmetric systems. As the isospin potential for the kaon is negligible (see eq. 11) the threshold energy will be only shifted by the isovector potential of the nucleons. The maximum effect will be seen for systems like lead where one gets

$$Q(\text{iso}) \approx E_n(p=0) - E_p(p=0) = -2g_{\rho N}R_{0,0} = -2\frac{g_{\rho N}^2}{m_\rho^2}\rho_{\text{iso}} \approx (16 \div 19) \text{ MeV} \frac{\rho_N}{\rho_0} \quad (42)$$

with the parameters of Table I. Hence, the charge exchange process will be a little bit suppressed in isospin asymmetric systems. The change is quite moderate but comparable with the in-medium shift of the Q -value for the kaon production process.

Antikaons will annihilate strongly due to the process $\bar{K}N \rightarrow \Lambda\pi$ which is exothermal in vacuum ($Q(\bar{K}N \rightarrow \Lambda\pi) \approx -180$ MeV). Also the Λ can annihilate via the process $\Lambda n \rightarrow NN\bar{K}$, but this process is endothermal ($Q(\Lambda n \rightarrow NN\bar{K}) \approx 317$ MeV) in vacuum and is usually neglected. Nevertheless, we expect rather strong in-medium modifications of these Q -values as the antikaon energy is involved which changes considerably in nuclear matter. The lower curves in Fig. 4 and 5 show these Q -values as a function of density. All models give an astonishingly similar strong behaviour in dense matter: $Q(\bar{K}N \rightarrow \Lambda\pi)$ is going up with density and crosses zero at $\rho \approx 1.5\rho_0$ while $Q(\Lambda n \rightarrow NN\bar{K})$ is decreasing rapidly. For the soft EOS, both Q -values reaches even similar values at high density of about 70 MeV regardless of the model used. This means that the annihilation of Λ 's is favoured in the medium while the annihilation of antikaons is suppressed. At very high density these processes are even equally possible. For the hard EOS (Fig. 5) the Q -values for the ChPT seem to saturate at high density at $Q(\bar{K}N \rightarrow \Lambda\pi) \approx 0$ MeV and $Q(\Lambda n \rightarrow NN\bar{K}) \approx 140$ MeV. On the contrary, the curves for the RMF model show a crossing, so that the situation is reversed and one gets $Q(\bar{K}N \rightarrow \Lambda\pi) \approx 115$ MeV and $Q(\Lambda n \rightarrow NN\bar{K}) \approx 20$ MeV. It would be interesting to examine how these in-medium effects of the annihilation process will influence the antikaon and Λ spectra in heavy ion collisions at subthreshold energy where they are most pronounced.

V. CONCLUSIONS AND OUTLOOK

The study of the in-medium properties of kaons and antikaons shows that it is important to link the models to the available data, here to the KN scattering data, and to take into account effects nonlinear in density. Then one gets rather similar predictions in the models discussed here for the energy of kaons and antikaons in nuclear matter up to a certain density, say $(1 - 2)\rho_0$. The kaon energy in matter is well determined by the low density theorem, while the antikaon energy is more model dependent. The threshold energy for the production of kaons is shifted up in dense matter, while the one for antikaons is considerable decreased. Also the threshold energy for the annihilation processes for antikaons and Λ 's

show strong in-medium modification and can even get similar values at high density. Hence, it will be important to study the process $\Lambda N \rightarrow NN\bar{K}$ in the medium which will enhance the number of produced antikaons in heavy ion collisions at subthreshold energy. This will also change the flow pattern of antikaons and Λ 's and will cause e.g. an antiflow of Λ 's for central rapidities. As the threshold energy for antikaon and Λ production as well as for annihilation become equal around $\rho \approx 3\rho_0$ the number of antikaons and Λ 's will be predicted to be equal in the dense zone of a heavy ion collision at subthreshold energy due to in-medium effects. The number of kaons will then be twice the number of antikaons due to strangeness conservation. This effect might be seen at midrapidity and high momenta.

Insofar, we have only discussed effects on the mean-field level which will cause shifts of the threshold energy and essentially modify the phase space of the reactions in the medium. Using Fermis golden rule, one can now implement these modifications into a dynamical model by simply changing the energy of all hadrons consistently and leaving the cross sections constant. Nevertheless, also the cross sections might change in the medium. For the process $NN \rightarrow NAK$, the NAK vertex has to be considered which vanishes on the mean field level. Hence, changes of the cross section are here of higher order. They have to be computed by taking into account the p-wave interactions of nucleons and kaons and will change the angular distribution of the produced kaons in heavy ion reactions. The investigation of these effects is an interesting task and will be considered in a forthcoming work.

ACKNOWLEDGMENTS

We like to thank Avraham Gal for initiating the study of the nonlinear behaviour of the Λ potential with density. We also thank Bo Jakobsson and Wolfram Weise for useful discussions and remarks. J.S. thanks Thomas Waas for the submission of the results of the coupled channel calculation for the kaon/antikaon energy in medium and Jörg Aichelin, Eckart Grosse, Christoph Hartnack, Che Ming Ko, Peter Senger and Andreas Wagner for illuminating conversations. I.N.M. is supported in part by the International Science Foun-

dation (Soros) grant N8Z000 and EU-INTAS grant 94-3405. Two of us (J.S. and I.N.M.) expresses their gratitude to the Niels Bohr Institute for their warm hospitality and financial support.

REFERENCES

- [1] A.E. Nelson and D.B. Kaplan, Phys. Lett. **B192**, 193 (1987)
- [2] M. Lutz, A. Steiner, W. Weise, Phys. Lett. **B278**, 29 (1992); Nucl. Phys. **A547**, 755 (1994)
- [3] G.E. Brown, C.-H. Lee, M. Rho, V. Thorsson, Nucl. Phys. **A567**, 937 (1994)
- [4] J. Schaffner, A. Gal, I.N. Mishustin, H. Stöcker, W. Greiner, Phys. Lett. **B334**, 268 (1994)
- [5] V. Koch, Phys. Lett. **B337**, 7 (1994)
- [6] T. Waas, N. Kaiser, W. Weise, Phys. Lett. **365B**, 12 (1996); **379B**, 34 (1996)
- [7] G.E. Brown, K. Kubodera, M. Rho, V. Thorsson, Phys. Lett. **B291**, 355 (1992)
V. Thorsson, M. Prakash, J.M. Lattimer, Nucl. Phys. **A572**, 693 (1994)
- [8] C.-H. Lee, H. Jung, D.-P. Min, M. Rho, Phys. Lett. **B326**, 14 (1994)
- [9] C.-H. Lee, G.E. Brown, D.-P. Min, M. Rho, Nucl. Phys. **A585**, 401 (1995)
- [10] T. Maruyama, H. Fujii, T. Muto, T. Tatsumi, Phys. Lett. **B337**, 19 (1994)
- [11] P.J. Ellis, R. Knorren, M. Prakash, Phys. Lett. **B349**, 11 (1995)
R. Knorren, M. Prakash, P.J. Ellis, Phys. Rev. **C52**, 3470 (1995)
- [12] J. Schaffner and I.N. Mishustin, Phys. Rev. **C53**, 1416 (1996)
- [13] D. Miskowiec et al. (KaoS collaboration, GSI), Phys. Rev. Lett. **72**, 3650 (1994)
P. Senger et al. (KaoS collaboration, GSI), Proceedings of the international conference on "Dynamical properties of hadrons in nuclear matter", Hirschegg 1995, p. 306
- [14] J. Aichelin, C.M. Ko, Phys. Rev. Lett. **55**, 2661 (1985)
- [15] C. Hartnack, J. Aichelin, H. Stöcker, W. Greiner, Phys. Rev. Lett. **72**, 3767 (1994)
C. Hartnack, L. Sehn, J. Jänicke, H. Stöcker, J. Aichelin, Nucl. Phys. **A580**, 643 (1994)

- [16] G.Q. Li, C.M. Ko, Phys. Lett. **B349**, 405 (1995)
- [17] J. Randrup, C.M. Ko, Nucl. Phys. **A343**, 519 (1980); Nucl. Phys. **A411**, 537 (1983)
- [18] W. Zwermann, Mod. Phys. Lett. **A3**, 251 (1988)
- [19] G. Batko, J. Randrup, T. Vetter, Nucl. Phys. **A54**, 761 (1992)
- [20] A. Sibirtsev, Phys. Lett. **B359**, 29 (1995)
- [21] T. Maruyama, W. Cassing, U. Mosel, S. Teis, K. Weber, Nucl. Phys. **A573**, 653 (1994)
- [22] X.S. Fang, C.M. Ko, G.Q. Li, Y.M. Zheng, Phys. Rev. **C49**, 608 (1994); Nucl. Phys. **A575**, 766 (1994)
- [23] G.Q. Li, C.M. Ko, B.A. Li, Phys. Rev. Lett. **74**, 235 (1995)
- [24] G.Q. Li, C.M. Ko, X.S. Fang, Phys. Lett. **B329**, 149 (1994)
- [25] A. Schröter, E. Berdermann, H. Geissel, P. Kienle, W. Koenig, A. Gillitzer, J. Homolka, F. Schumacher, H. Ströher, B. Povh, Nucl. Phys. **A553**, 775c (1993); Z. Phys. **A350**, 101 (1994); R. Barth et al. (KaoS collaboration), GSI report 10-95, p. 9; P. Senger, private communication
- [26] B.D. Serot and J.D. Walecka, Adv. in Nucl. Phys. **16**, 1 (1986)
B.D. Serot, Rep. Prog. Phys. **55**, 1855 (1992)
- [27] P.-G. Reinhard, Rep. Prog. Phys. **52**, 439 (1989)
- [28] J. Boguta and A.R. Bodmer, Nucl. Phys. **A292**, 413 (1977)
J. Boguta and H. Stöcker, Phys. Lett. **B120**, 289 (1983)
- [29] P.-G. Reinhard, Z. Phys. **A329**, 257 (1988)
- [30] M. Rufa, P.-G. Reinhard, J. Maruhn, W. Greiner, M.R. Strayer, Phys. Rev. **C38**, 390 (1988)

- [31] M.M. Sharma, M.A. Nagarajan, P. Ring, Phys. Lett. **B312**, 377 (1993)
- [32] A.R. Bodmer and C.E. Price, Nucl. Phys. **505**, 123 (1989)
- [33] A.R. Bodmer, Nucl. Phys. **A526**, 703 (1991)
- [34] S. Gmuca, J. Phys. **G17**, 1115 (1991); Z. Phys. **A342**, 387 (1991); Nucl. Phys. **A547**, 447 (1992)
- [35] Y. Sugahara and H. Toki, Nucl. Phys. **A579**, 557 (1994)
- [36] R. Brockmann, W. Weise, Phys. Lett. **69B**, 167 (1977)
 J. Boguta, S. Bohrmann, Phys. Lett. **102B**, 93 (1981)
 M. Rufa, H. Stöcker, P.-G. Reinhard, J. Maruhn, W. Greiner, J. Phys. **G13**, L143 (1987)
 J. Mareš, J. Žofka, Z. Phys. **A333**, 209 (1989)
 M. Rufa, J. Schaffner, J. Maruhn, H. Stöcker, W. Greiner, P.-G. Reinhard, Phys. Rev. **C42**, 2469 (1990)
- [37] N.K. Glendenning and S.A. Moszkowski, Phys. Rev. Lett. **67**, 2414 (1991)
- [38] J. Schaffner, C. Greiner, H. Stöcker, Phys. Rev. **C46**, 322 (1992)
- [39] C.B. Dover, G.E. Walker, Phys. Rep. 89, 1 (1982)
- [40] J.V. Noble, Phys. Lett. **89B**, 325 (1980)
- [41] D.J. Millener, C.B. Dover, A. Gal, Phys. Rev. **C38**, 2700 (1988)
- [42] T. Barnes and E.S. Swanson, Phys. Rev. **C49**, 1166 (1994)
- [43] R. Weiss, J. Aclander, J. Alster, M. Barakat, S. Bart, R.E. Chrien, R.A. Krauss, K. Johnston, I. Mardor, Y. Mardor, S. MayTal-Beck, E. Piassetzky, P.H. Pile, R. Sawafta, H. Seyfarth, R.L. Stearns, R.J. Sutter, A.I. Yavin, Phys. Rev. **C49**, 2569 (1994)
- [44] E. Friedman, A. Gal, C.J. Batty, Phys. Lett. **B308**, 6 (1993); Nucl. Phys. **A579**, 518

(1994)

- [45] P.B. Siegel and W. Weise, Phys. Rev. **C38**, 2221 (1988)
- [46] R. Büttgen, K. Holinde, A. Müller-Groeling, J. Speth, P. Wyborny, Nucl. Phys. **A506**, 586 (1990)
A. Müller-Groeling, K. Holinde, J. Speth, Nucl. Phys. **A513**, 557 (1990)
- [47] N. Kaiser, P.B. Siegel, W. Weise, Nucl.Phys. **A594**, 325 (1995)
- [48] J. Cohen, Phys. Rev. **C39**, 2285 (1989)
- [49] R. Machleidt, K. Holinde, C. Elster, Phys. Rep. **149**, 1 (1987)
- [50] G.E. Brown and M. Rho, Nucl. Phys. **A596**, 503 (1996)
- [51] G.E. Brown and M. Rho, Phys. Rep. **269**, 333 (1996)

TABLES

TABLE I. The coupling constants of the parameter sets used. The vector coupling constant for the Λ are taken from SU(6)-relations. The coupling constants of the kaons to the σ - and δ -meson are fixed by the s-wave KN-scattering lengths. The vector coupling constants are chosen from SU(3)-relations. The parameters for the scalar and vector selfinteraction terms are not given, they can be found in the corresponding references.

Set	NL-Z	NL-SH	PL-Z	PL-40	TM1	TM2
Ref.	[30]	[31]	[29]	[29]	[35]	[35]
$g_{\sigma N}$	10.0553	10.4440	10.4262	10.0514	10.0289	11.4694
$g_{\omega N}$	12.9086	12.9450	13.3415	12.8861	12.6139	14.6377
$g_{\rho N}$	4.8494	4.3830	4.5592	4.8101	4.6322	4.6783
$g_{\sigma\Lambda}$	6.23	6.47	6.41	6.20	6.21	7.15
$g_{\omega\Lambda}$	8.61	8.63	8.89	8.59	8.41	9.76
$g_{\sigma K}$	1.85	2.05	2.20	2.27	1.93	2.27
$g_{\omega K}$	3.02	3.02	3.02	3.02	3.02	3.02
$g_{\rho K}$	3.02	3.02	3.02	3.02	3.02	3.02
$g_{\delta K}$	6.37	5.59	5.89	6.31	5.87	5.94

FIGURES

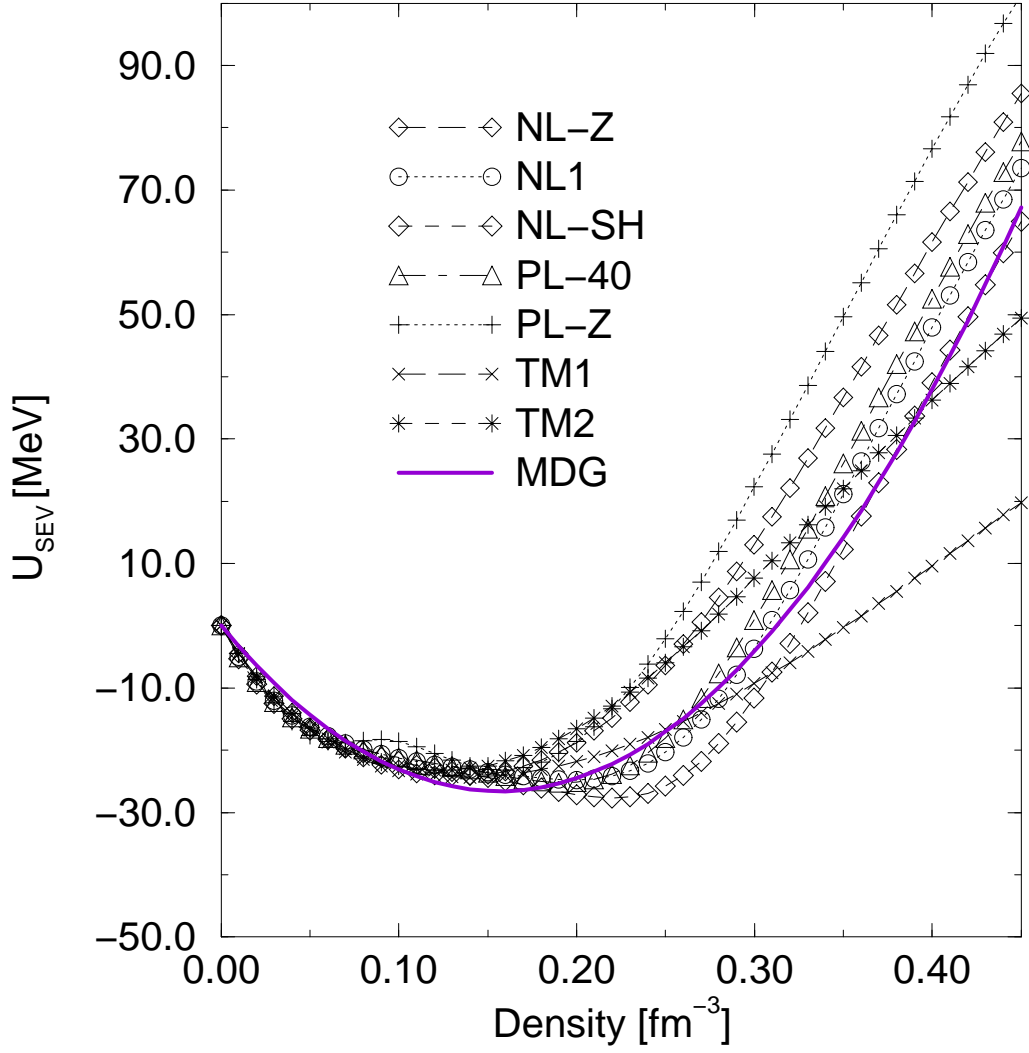


FIG. 1. The Schrödinger equivalent potential of the Λ for several parameter sets of the RMF model as a function of density. The curve labelled MDG is the non-relativistic potential fit to hypernuclear data of Dover, Millener and Gal [41].

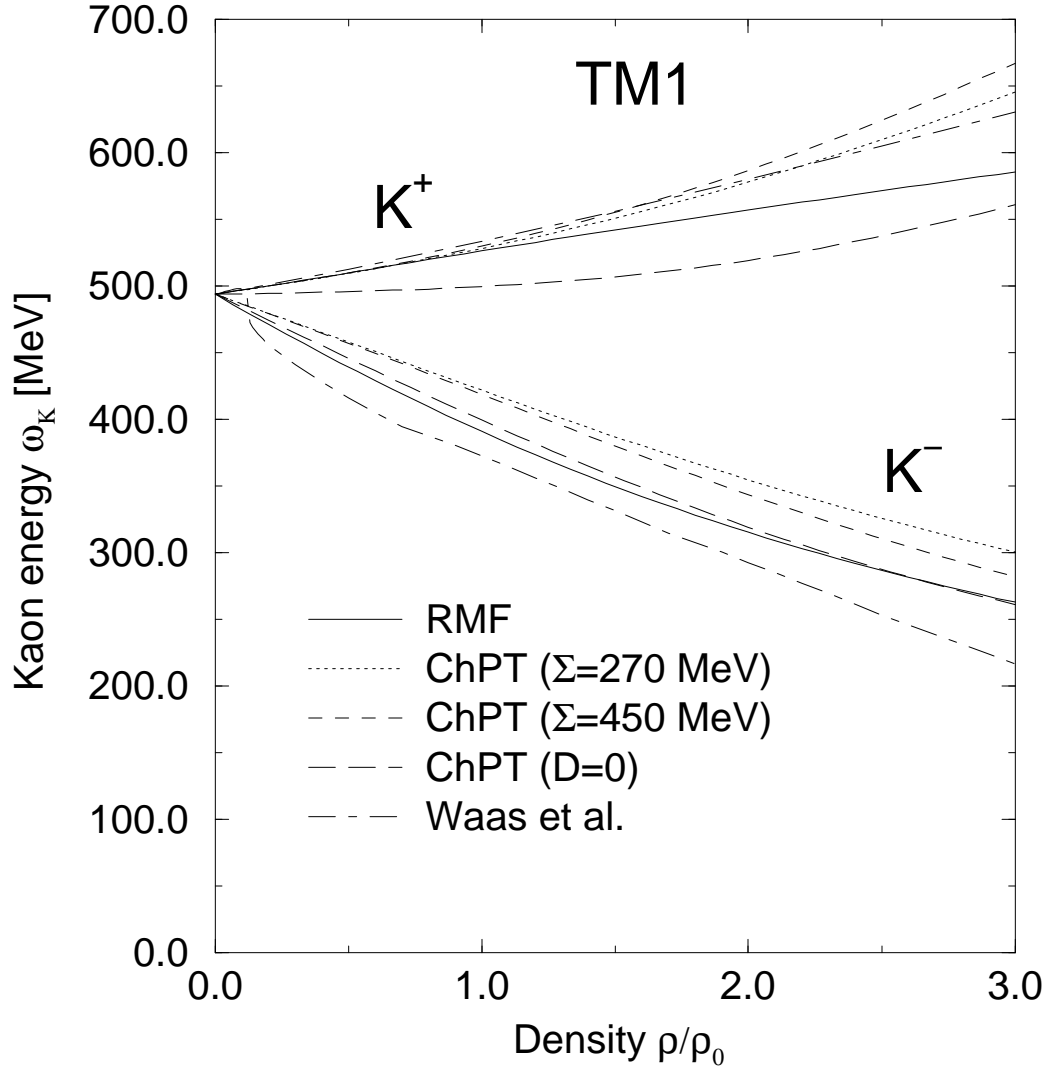


FIG. 2. The energy of kaons and antikaons in nuclear matter as function of density for the soft EOS (parameter set TM1).

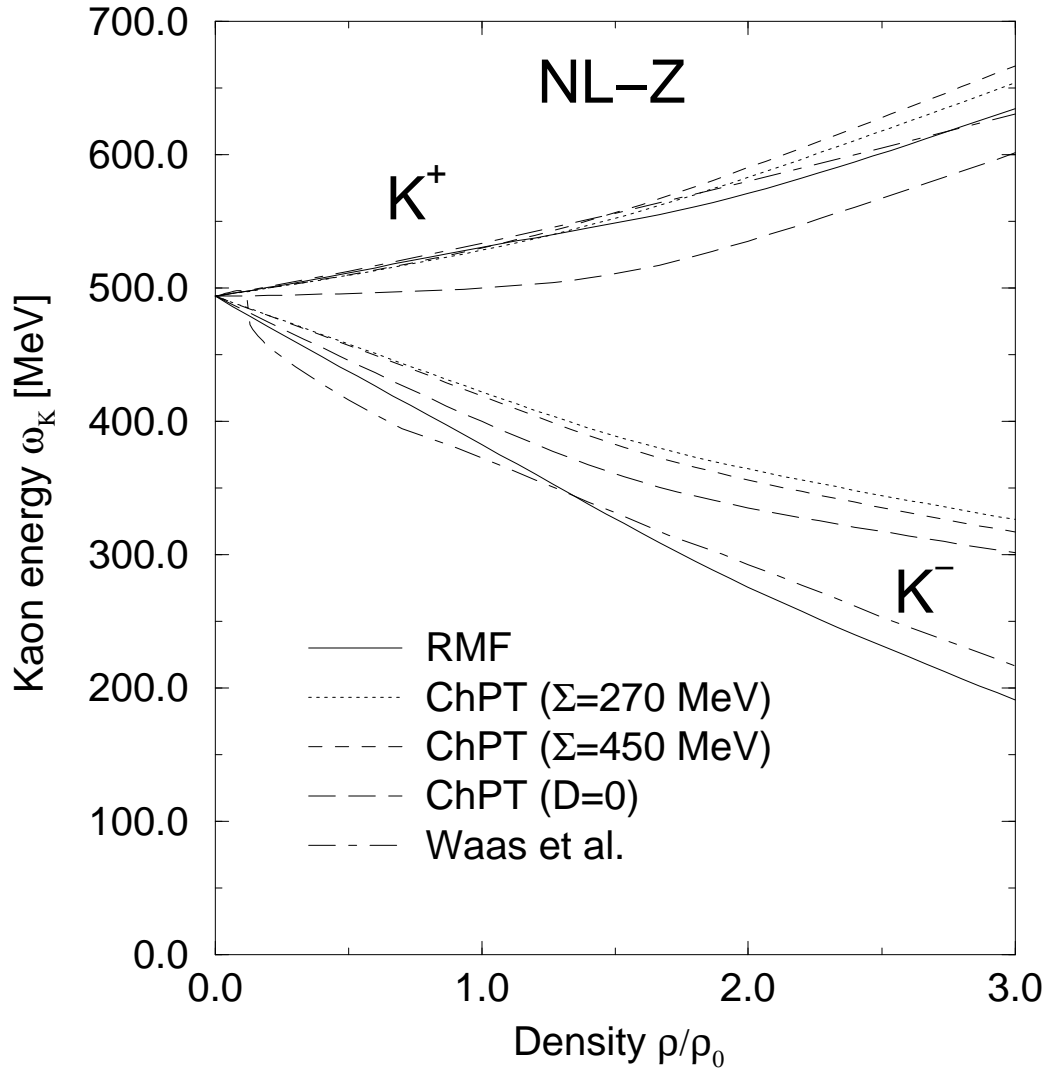


FIG. 3. The same as Fig. 2 for the hard EOS (parameter set NL-Z).

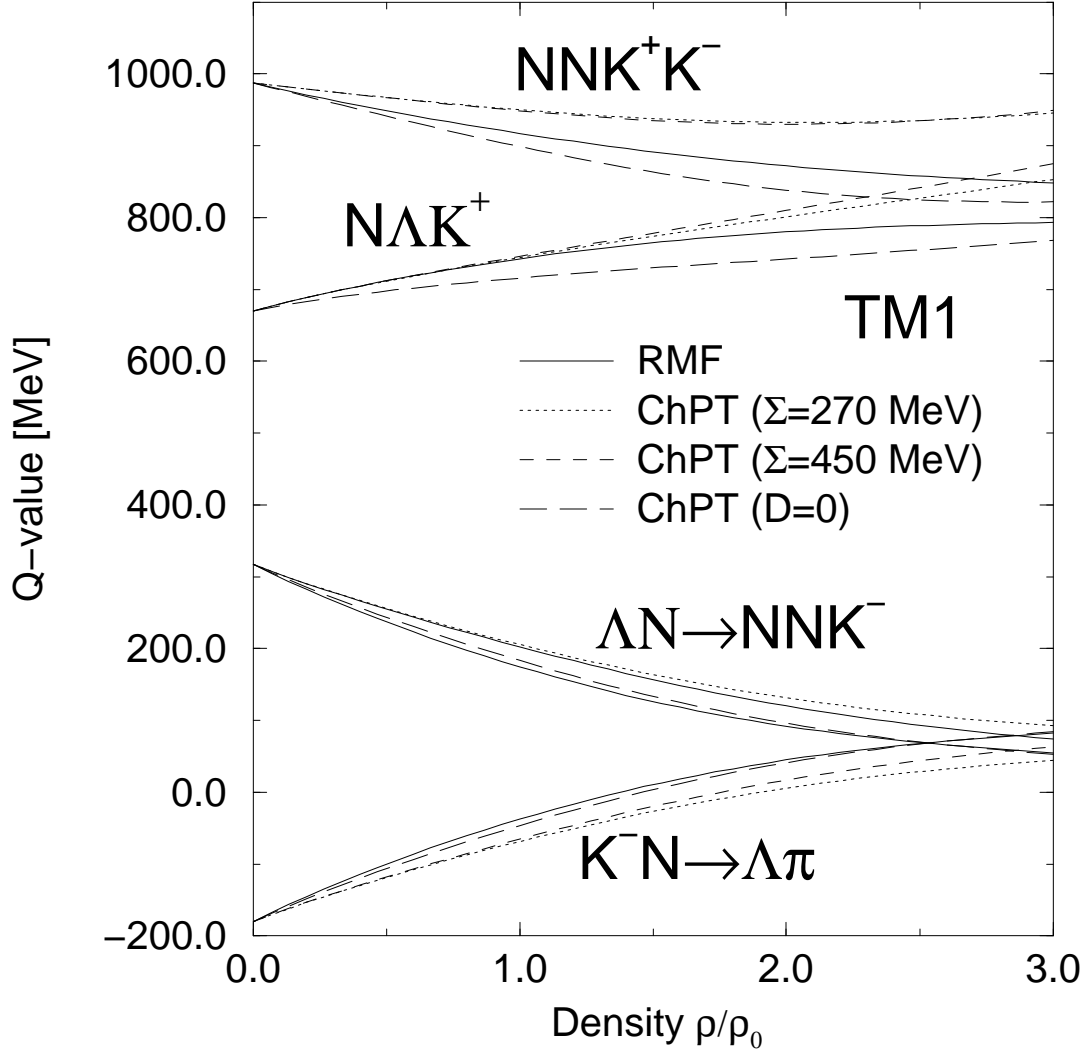


FIG. 4. The Q -values of the production processes of kaons and antikaons (the two upper bunches of curves) and the annihilation processes of antikaons and Λ 's (lower bunches of curves) versus the density for the soft EOS.

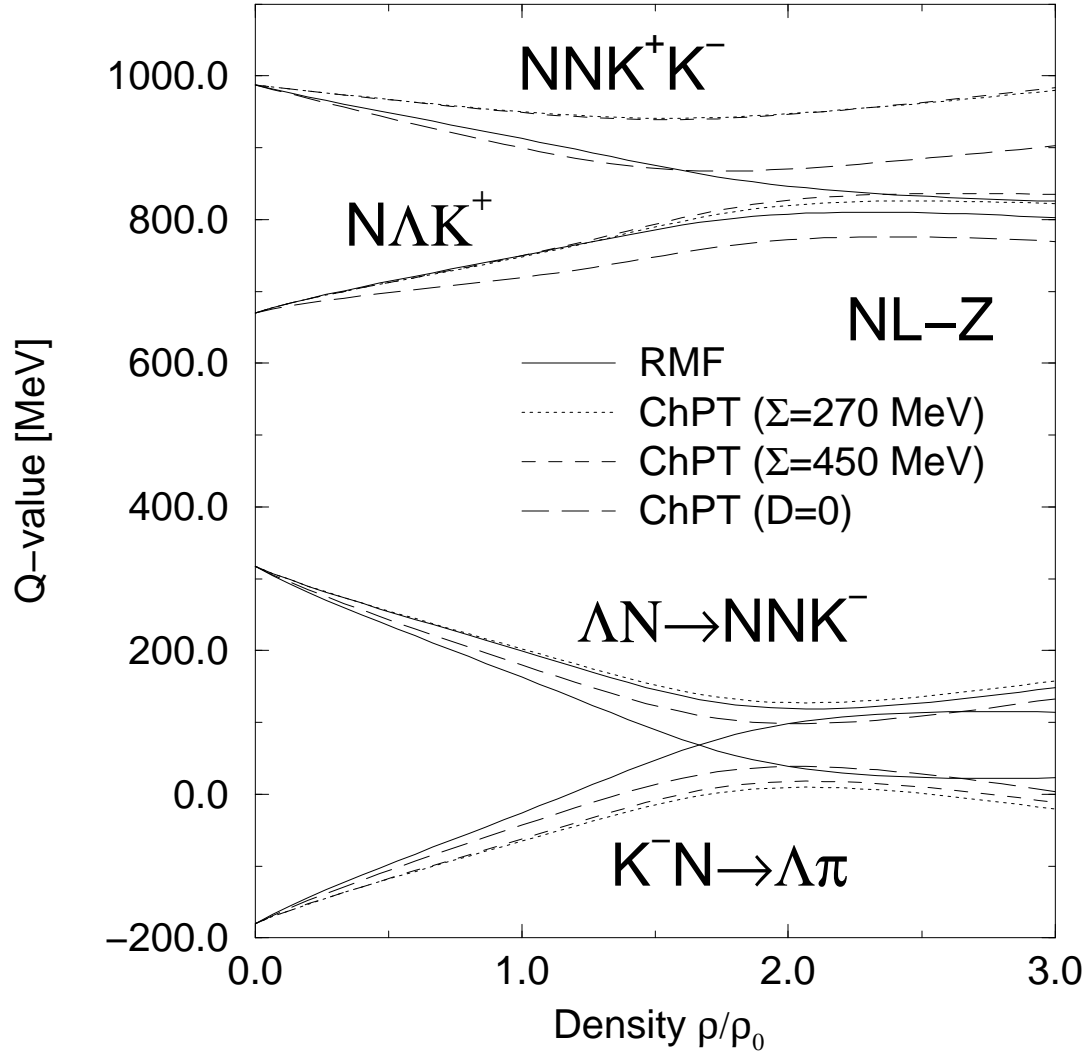


FIG. 5. The same as Fig. 4 for the hard EOS.